Higher Order Assembly of Microtubules by Counter-ions: From Hexagonal Bundles to Living Necklaces

Daniel J. Needleman,[1-4] Miguel A. Ojeda-Lopez,[1-4] Uri Raviv,[1-4] Herbert P. Miller,[3,4] Leslie Wilson,[3,4] and Cyrus R. Safinya[1-4]

Departments of [1]Materials, [2]Physics, and [3]Molecular, Cellular, and Developmental Biology, and [4]Biomolecular Science and Engineering Program, University of California, Santa Barbara, CA 93106

Cellular factors tightly regulate the architecture of bundles of filamentous cytoskeletal proteins, giving rise to assemblies with distinct morphologies and physical properties, and a similar control of the supramolecular organization of nanotubes and nanorods in synthetic materials is highly desirable. However, it is unknown what principles determine how macromolecular interactions lead to assemblies with defined morphologies. In this study we present our findings on the assembly behavior of multivalent cations and microtubules (MTs), a cytoskeletal polymer and model nanoscale tubule (*1*). Tightly packed hexagonal bundles with controllable diameters are observed for large tri-, tetra-, and pentavalent counterions [Figure 1]. Unexpectedly, in the presence of small divalent cations, we have discovered a living necklace bundle phase, comprised of dynamical assemblies of MT nematic membranes with linear, branched, and loop topologies [Figure 1]. The morphologically distinct MT assemblies give insight into general features of bundle formation and may be used as templates for miniaturized materials with applications in nanotechnology and biotechnology.

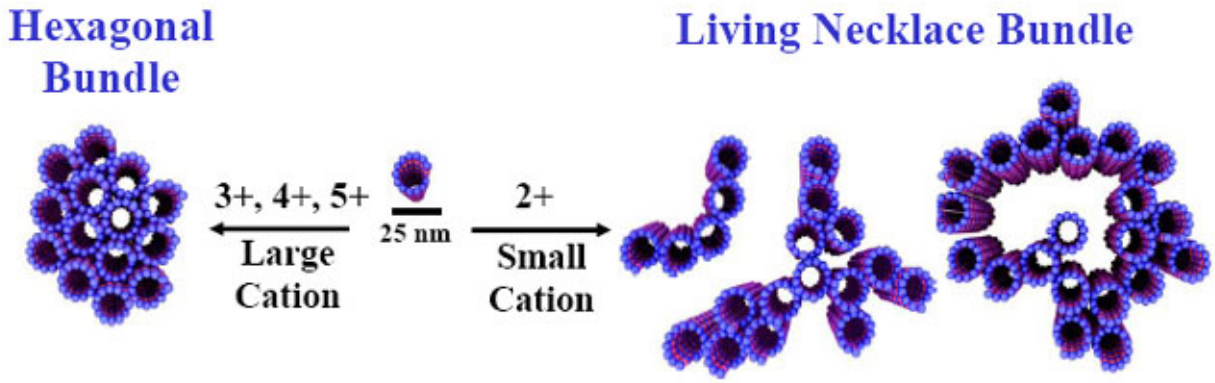

Figure 1. Three dimensional schematics of higher order assembly of nanometer scale microtubules. Large tri-, tetra-, and pentavalent cations lead to the formation of hexagonal bundles (left). Small divalent cations lead to the living necklace bundles with linear, branched, and loop morphologies (right). The distinct bundle phases allow for tailored applications in miniaturized materials requiring high volume (hexagonal bundles) or high surface area (necklace bundles).

The structure of these supramolecular assemblies was elucidated on length scales from subnanometer to micrometer with synchrotron x-ray diffraction, transmission electron microscopy, and differential interference contrast microscopy. The mesoscopic structure of MT bundles is shown in video-enhanced DIC images of Figure 2A. The bundles formed in the

presence of large, tri-, tetra-, and pentavalent cations, (such as Spermine 4+) appear thick and curved, while bundles formed with small divalent cations (such as Ba 2+) are straight. Individual MTs can easily be resolved with TEM, which clearly shows that bundles formed with large multivalent ions are thick, with MTs tightly packed into a hexagonal array [Figure 2B]. A radically different bundle structure, which we refer to as the living necklace bundle phase of MTs, is observed when the condensing ions are small, divalent cations. On the nanometer scale, TEM shows that these necklace bundles are highly flexible in cross-section, giving rise to topologically distinct linear, branched, and loop morphologies [Figure 2C].

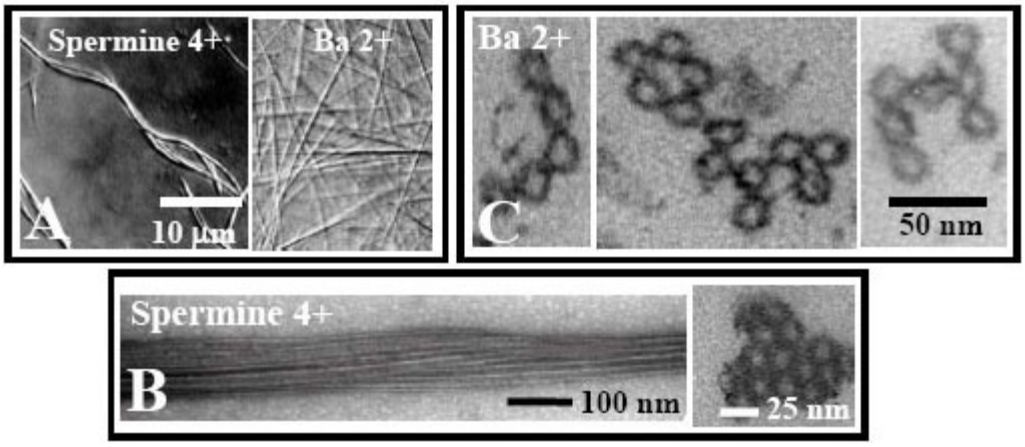

Figure 2. (A) Differential interference contrast (DIC) optical micrographs of hexagonal microtubule (MT) bundles with 4+ (5 mM spermine) and 2+ (100 mM $BaCl_2$). (B) (left) whole mount TEM side view of hexagonal MT bundles (10 mM spermine) and (right) plastic embedded TEM cross section. (C) Plastic embedded TEM cross sections of bundles with 100 mM $BaCl_2$ showing (left) linear, (center) loop-like and (right) branched morphologies.

We have performed a series of synchrotron small angle x-ray scattering and diffraction (SAXRD) experiments at SSRL on beamline 4-2 to gain further insight into the angstrom scale structure of these MT bundles. Figure 3A shows representative raw SAXRD scans that have been integrated 360° from a powder pattern on a 2D detector, and are displayed as a function of the scattering vector, *q*. To quantitatively model this data, we have subtracted a background that consists of a polynomial that passes through the minimum of the scattering intensities [Figure 3B]. The MTs are modeled as hollow cylinders with an outer radius of 12.9 nm and a wall thickness of 3.2 nm [Fig 3B, No Cation]. The tight bundle phase, for ions with valence five to three, are modeled as a collection of hollow cylinders, with the dimensions given above, packed into a hexagonal lattice. These bundles are finite-size, hexagonal, columnar liquid crystals *(2)*. The average bundle thickness can be determined from the peak width using Warren's approximation *(3)*. As the charge of the condensing ion decreases from 5+, to 4+, to 3+ the MT center-to-center distance increases and the bundle size decreases [Figure 3C]. SAXRD scans of bundles assembled with divalent ions display very broad peaks [Figure 3A, 2+], in contrast with the tight bundle phase. Indeed, instead of the hexagonal bundles observed with larger multivalent ions, detailed analysis shows that this SAXRD data can be quantitatively modeled as arising from a dimer of MTs. The only fit parameter is the MT-MT spacing [Figure 3C, left, Ca^{2+}, Ba^{2+}, Sr^{2+}]. The SAXRD data combined with TEM results [Figure 2C] show that these living bundles are finite size, locally two dimensional membranes with

nematic ordering, i.e. they consist of rod-like subunits (MTs) that spontaneously break symmetry by orienting but show only short range positional order. These bundles are an experimental realization of nematic membranes which have recently been predicted as a new universality class of membrane *(4)*.

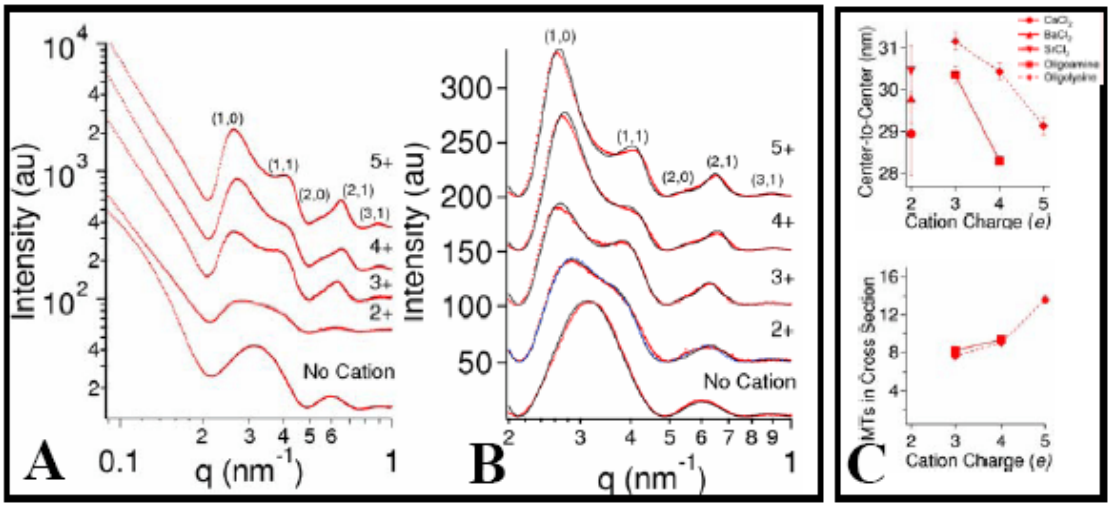

Figure 3. (A) Raw SAXRD scattering data for MTs with no cation, (2+) 115 mM $BaCl_2$, (3+) 15 mM spermidine, (4+) 5 mM spermine, or (5+) 5 mM oligolysine-five with hexagonal bundle peaks indexed. (B) Data in (A) after background subtraction (dots) with fitted model scattering curves (lines). (C) Summary of SAXRD scattering fit parameters of MT bundles with $CaCl_2$, $SrCl_2$, $BaCl_2$, oligoamines (spermidine and spermine), and oligolysines.

The bundles studied here have been created through nonspecific interactions so the living necklace bundle phase is likely to be a general feature of rod-like polyelectrolytes, as the hexagonal bundle phase is. These living necklace bundles are highly asymmetric self-assembled membranes of MTs with nematic in plane ordering and varying topology. The model system studied here may be viewed as a step toward understanding how varying microscopic interactions lead to the wide variety of MT bundles observed *in vivo (5)*. In addition to providing insight into the fundamental physics of rod-like polyelectrolytes and the general determinants of bundle structure, the control of bundle morphology demonstrated here may help to assemble nanostructures for engineering and biomedical applications.

Supported by NSF grant DMR 0203755 and NIH grants GM-59288 and NS-13560. Further supported was provided by NSF CTS 0404444, CTS 0103516, and the Department of Energy's Office of Basic Energy Sciences under Contract No. W-7405-ENG-36 with the University of California. U. Raviv acknowledges the support of the International Human Frontier Science Program Organization. The Materials Research Science and Engineering Center at UCSB is supported by NSF DMR-0080034. Portions of this research were carried out at the Stanford Synchrotron Radiation Laboratory, a national user facility operated by Stanford University on behalf of the U.S. Department of Energy, Office of Basic Energy Sciences. The SSRL Structural Molecular Biology Program is supported by the Department of

Energy, Office of Biological and Environmental Research, and by the National Institutes of Health, National Center for Research Resources, Biomedical Technology Program.

Primary Citation:

Needleman, D.J., Ojeda-Lopez, M.A., Raviv, U., Miller, H.P., Wilson, L., Safinya, C.R. (2004) *Proc. Nat. Ac. Sci.* **101**, 16099-16103

References:

1. Needleman, D.J., Ojeda-Lopez, M.A., Raviv, U., Miller, H.P., Wilson, L., Safinya, C.R. (2004) *Proc. Nat. Ac. Sci.* **101**, 16099-16103
2. Selinger, J.V., Bruinsma, R.F. (1991) *Phys. Rev. A* **43**, 2910-2921
3. Warren, B.E. (1941) *Phys. Rev.* **59**, 693-698
4. Xing, X., Mukhopadhyay, R., Lubensky, T.C., Radzihovsky, L. (2003) *Phys. Rev. E* **68**, 021108
5. *Cell Movements*, D. Bray (Taylor & Francis, New York, 2001)

SSRL is supported by the Department of Energy, Office of Basic Energy Sciences. The SSRL Structural Molecular Biology Program is supported by the Department of Energy, Office of Biological and Environmental Research, and by the National Institutes of Health, National Center for Research Resources, Biomedical Technology Program, and the National Institute of General Medical Sciences.